Synthesis and Structural Analysis of $Sr_{5.8}La_{4.4}Ti_{7.8}S_{24}O_4$ and $La_{14}Ti_8S_{33}O_4$: Two New Oxysulfides Containing a Common $^2_\infty[(Ti_4S_2O_4)(TiS_6)_{4/2}]^{12-}$ Layer

Louis J. Tranchitella, James C. Fettinger, and Bryan W. Eichhorn*

Center for Superconductivity Research and Department of Chemistry and Biochemistry, University of Maryland, College Park, Maryland 20742

Received January 2, 1996. Revised Manuscript Received May 21, 1996[⊗]

Two new titanium oxysulfides $Sr_{5.8}La_{4.4}Ti_{7.8}S_{24}O_4$ and $La_{14}Ti_8S_{33}O_4$ were prepared by high-temperature methods (925−950 °C; ∼ 90−104 h) from stoichiometric ratios of SrS, La_2S_3, Ti, S, and TiO_2 or La_2O_3 (or SrO for $Sr_{5.8}La_{4.4}Ti_{7.8}S_{24}O_4$) oxygen sources. The sample crystallinity and purity was greatly enhanced when $LaCl_3$ fluxes were employed. The compounds were characterized by single-crystal and powder (Rietveld profile analysis) X-ray diffraction studies and EDX analysis. Both compounds are black insulators (all Ti^{4+}) and contain a common $^2_\infty[(Ti_4S_2O_4)(TiS_6)_{4/2}]^{-12}$ layer despite the difference in composition and crystal symmetry. For $La_{14}Ti_8S_{33}O_4$, these layers are separated by TiS_6 octahedra and 8- and 9-coordinate La−S polyhedra. For $Sr_{5.8}La_{4.4}Ti_{7.8}S_{24}O_4$, the layers are separated by a TiS_6 octahedron and two disordered $Ti_{1-x}Sr_xS_6$ octahedra. La and Sr are also disordered on an interlayer nine-coordinate site. Crystal data (153 K): $Sr_{5.8}La_{4.4}Ti_{7.8}S_{24}O_4$, tetragonal, space group $P4/mmm$ $a = 10.569(3)$, $c = 8.516(4)$ Å, $V = 951.4(5)$ Å^3, $Z = 1$, $R(F) = 4.28\%$, and $R_w(F^2) = 10.39\%$. For $La_{14}Ti_8S_{33}O_4$, monoclinic, space group $C2/m$, $a = 14.904(1)$, $b = 14.736(1)$, $c = 12.278(1)$ Å, $\beta = 112.773(5)°$, $V = 2486.2(3)$ Å^3, $Z = 2$, $R(F) = 3.92\%$, and $R_w(F^2) = 10.00\%$.

Introduction

In contrast to the large number of ternary oxides and the growing number of ternary sulfides of the early transition metals, the corresponding number of oxysulfides are few.[1−6] The oxysulfide class of compounds are distinct from the sulfoxides (i.e. the sulfates, sulfites, thiosulfates, etc.) in that there are no S−O bonds. Instead, the lattices are composed of S^{2-} and O^{2-} ions bound directly to metal cations. Although few in number, early-transition-metal oxysulfides are of interest for use as cathode materials in solid-state batteries,[7−9] phosphors in imaging systems,[10,11] and fuel desulfurizing agents.[12]

For the sulfur-rich oxysulfides, the structures are quite similar to the sulfide phases as expected. For example, $MoS_{2-x}O_x$ thin films appear to retain the 2H-MoS_2 type structure[9] and the $Ba_6Ti_5S_{15}O$[5] structure closely resembles that of $BaTiS_3$. With higher oxygen contents, the structures are quite different from the sulfides as exemplified by the recently reported compounds $La_6Ti_5S_8O_5$ and $La_4Ti_3S_4O_8$.[6] For early-transition-metal oxysulfides, the oxide ions are almost always bound to the transition metals. Several mixed-transition-metal coordination environments have been observed including $TiSO_5$, TiS_3O_3, TiS_4O_2, TiS_5O, VOS_3, and VS_2O_2.[5,6,13]

We report here the syntheses and structures of two new oxysulfides of formulas $Sr_{5.8}La_{4.4}Ti_{7.8}S_{24}O_4$ and $La_{14}Ti_8S_{33}O_4$. Despite the differences in compound compositions and crystal symmetry, both phases have a common $^2_\infty[(Ti_4S_2O_4)(TiS_6)_{4/2}]^{-12}$ oxysulfide layer containing $Ti_4S_2O_4$ clusters. Immediately prior to the submission of this paper, Deudon, et al.[14] reported the crystal structure of $La_{20}Ti_{11}S_{44}O_4$ which also contains $Ti_4S_2O_4$ clusters in a slightly different layered structure. The similarities of these and other related phases appear to be driven by the stability of the oxysulfide cluster units.

Experimental Section

Syntheses. All reagents were purchased from CERAC and used without further purification. $Sr_{5.8}La_{4.4}Ti_{7.8}S_{24}O_4$ was prepared as a bulk phase from stoichiometric amounts of SrS, La_2S_3, Ti, S, and either SrO or TiO_2 as the oxide source. $LaCl_3$ was added (30% by weight) as a flux. The starting materials were ground in an N_2 drybox and loaded in a carbon-coated silica ampule. The ampule was sealed under vacuum and fired at 925 °C for 3 days. The ampule was cooled to 850 °C at 3 °C/h and then cooled to room temperature in 3 h. The sample

[⊗] Abstract published in *Advance ACS Abstracts,* July 15, 1996.

(1) Dugué, J.; Vovan, T.; Villers, J. *Acta Crystallogr.* **1980**, *B36*, 1291.
(2) Wintenberger, M.; Dugué, J.; Guittard, M.; Dung, N. H.; Tien, V. V. *J. Solid State Chem.* **1987**, *70*, 295.
(3) Dugué, J.; Vovan, T.; Laruelle, P. *Acta Crystallogr.* **1985**, *C41*, 1146.
(4) Brennan, T. D.; Aleandri, L. E.; Ibers, J. A. *J. Solid State Chem.* **1991**, *91*, 312.
(5) Sutorik, A. C.; Kanatzidas, M. G. *Chem. Mater.* **1994**, *10*, 1700.
(6) Cody, J. A.; Ibers, J. A. *J. Solid State Chem.* **1995**, *114*, 406.
(7) Ouvrard, G.; Tchangbedji, G.; Deniard, P.; Prouzet, E. *J. Power Sources* **1995**, *54*, 246.
(8) Schmidt, E.; Meunier, G.; Levasseur, A. *Solid State Ionics* **1995**, *76*, 243.
(9) Levasseur, A.; Schmidt, E.; Meunier, G.; Gonbeau, D.; Benoist, L.; Pfisterguillouzo, G. *J. Power Sources* **1995**, *54*, 352.
(10) Bizzak, D. J.; Chyu, M. K. *Rev. Sci. Instrum.* **1994**, *65*, 102.
(11) Bizzak, D. J.; Chyu, M. K. *Int. J. Heat and Mass Trans.* **1995**, *38*, 1995.
(12) Zhong, S. L.; Hepworth, M. T. *Energy Fuel* **1994**, *8*, 276.
(13) Litteer, B.; Fettinger, J. C.; Eichhorn, B. W., submitted for publication.
(14) Deudon, C.; Meerschaut, A.; Cario, L.; Rouxel, J. *J. Solid State Chem.* **1995**, *120*, 164.

S0897-4756(96)00001-4 CCC: $12.00

was washed with ethanol and filtered to dissolve and remove the $LaCl_3$ flux. The reaction yielded a black crystalline powder and small black single crystals (approximately 0.01 mm on edge).

Single crystals of $Sr_{5.8}La_{4.4}Ti_{7.8}S_{24}O_4$ were initially prepared from SrS, La_2S_3, Ti, and S in a 3:1:5:9 molar ratio in the presence of 20 wt % $SrCl_2$ flux. The starting materials were processed as above and fired at 925 °C for 3.5 days. The reaction was cooled to 800 °C at 3 °C/h and then cooled to room temperature in 3 h. The sample was washed with water and filtered to dissolve and remove the $SrCl_2$ flux. The reaction yielded a black, crystalline powder (essentially single-phase $(LaS)_{1+x}CrS_2$ type compound)[15,16] with small cubelike single crystals (approximately 0.3 mm on edge) of the title compound. The source of oxygen is unknown.

Single-phase samples of $La_{14}Ti_8S_{33}O_4$ were prepared as a bulk phase from a 7:2:6:12 ratio of La_2S_3, TiO_2, Ti, and S (CERAC Inorganics). $LaCl_3$ was added (20% by weight) as a flux. The starting materials were ground in an N_2 drybox and loaded in a carbon-coated silica ampule. The ampule was sealed under vacuum and ramped to 950 °C at 0.3 °C/min and fired and 950 °C for 104 h. The sample was then cooled to 850 °C at 3 °C/h and then cooled to room temperature at 5 °C/min. The mixture was washed with ethanol and filtered to dissolve and remove the $LaCl_3$ flux. The reaction yielded a black crystalline powder and small black single crystals (approximately 0.01 mm on edge).

Single crystals of $La_{14}Ti_8S_{33}O_4$ were originally prepared from SrS, La_2S_3, Ti, and S (CERAC Inorganics) in a 1:2:5:8 molar ratio. $LaCl_3$ was added (20% by weight) as a flux. The reactants were ground in an N_2 drybox and loaded in a carbon-coated silica ampule. The ampule was sealed under vacuum and fired at 950 °C for 3.5 days. The ampule was cooled to 850 °C at 3 °C/h and then cooled to room temperature in 3 h. The sample was washed and filtered with ethanol to dissolve and remove the $LaCl_3$ flux. The reaction yielded a black crystalline powder (essentially single-phase $La_6Ti_5S_{16}$, a $(LaS)_{1+x}$-TiS_2 type compound),[15,16] with small blocklike single crystals (approximately 0.1 mm on edge). The source of oxygen is unknown.

Single crystals were analyzed by energy-dispersive X-ray analysis (EDX) on a JEOL 840 scanning electron microscope. Samples from the three different preparations of $Sr_{5.8}La_{4.4}$-$Ti_{7.8}S_{24}O_4$ contained Sr, La, Ti, and S; however, there were apparent variations in the peak heights. EDX on samples from the different preparations of $La_{14}Ti_8S_{33}O_4$ contained La, Ti, and S but no Sr. The EDX analyses of both phases were complicated by the overlap of the La and Ti peaks which precluded semiquantitative analysis.

Bond valence analyses were performed using the methods and data of Brese and O'Keefe.[17]

Structural Determinations. *$Sr_{5.8}La_{4.4}Ti_{7.8}S_{24}O_4$*: A shiny black crystal with dimensions 0.31 × 0.28 × 0.28 mm was placed on the Enraf-Nonius CAD-4 diffractometer. The crystals' final cell parameters and crystal orientation matrix were determined from 25 reflections in the range $39.3° < 2\theta < 42.1°$; these constants were confirmed with axial photographs. Data were collected [Mo Kα] with $\omega/2\theta$ scans over the range $2.7° < \theta < 27.5°$ with a scan width of $(1.24 + 0.88 \tan \theta)°$ and a variable scan speed of 2.1−4.1° min^{-1}. Seven ψ-scan reflections were collected over the range $5.2° < \theta < 21.1°$; the absorption correction was applied with transmission factors ranging from 0.4835 to 0.9960; average correction 0.7218. Data were corrected for Lorentz and polarization factors and absorption and reduced to observed structure-factor amplitudes using the program package NRCVAX.[18] The structure was initially determined in *P*222 (No. 16) of the orthorhombic class. The program MISSYM[18] examined the atomic positions and indicated the existence of a 4-fold axis and an inversion center indicating the tetragonal system. The structure was subsequently determined in *P*4/*mmm* (No. 123) and refined with SHELXL-93.[19] Refinement of the structure converged well, and it was apparent that three of the sites were composed of mixed occupancy atoms. Many possibilities were attempted and SUMP instructions were included to force the overall charge to zero. The structure was refined to convergence with $R(F) = 5.35\%$, $wR(F^2) = 11.13\%$ and GOF = 1.032 for all 693 unique reflections [$R(F) = 4.28\%$, $wR(F^2) = 10.39\%$ for those 553 data with $F_o > 4\sigma(F_o)$]. A final difference-Fourier map possessed large peaks within 1 Å of the heavy atoms and $|\Delta\rho| \leq 1.78$ e Å^{-3}.

$La_{14}Ti_8S_{33}O_4$: A shiny black-capped pyramid-shaped crystal with dimensions 0.125 × 0.10 × 0.025 mm was placed on the Enraf-Nonius CAD-4 diffractometer. The crystals' final cell parameters and crystal orientation matrix were determined from 25 reflections in the range $17.6° < \theta < 22.0°$; these constants were confirmed with axial photographs. Data were collected [Mo Kα] with $\omega/2\theta$ scans over the range $2.0° < \theta < 25.0°$ with a scan width of $(0.38 + 0.64 \tan \theta)°$ and a variable scan speed of 2.3−3.3° min^{-1}. Nine ψ-scan reflections were collected over the range $9.1° < \theta < 21.3°$ resulting in a max:min transmission correction of 0.2914:0.1434. Data were corrected for Lorentz and polarization factors (XCAD4) and absorption (SHELXTL). The original data indicated a monoclinic C-centered crystal system which was confirmed with axial photos. Systematic absences indicated the monoclinic centrosymmetric space group *C*2/*m* (No. 12) or the noncentrosymmetric space groups *C*2 (No. 5) or *C*m (No. 8). Intensity statistics favored the centrosymmetric possibility and it was in this space group, *C*2/*m*, that the structure was successfully refined. The structure was initially solved in a triclinic setting giving seven lanthanum atoms and five titanium atoms, and SHELXL was used to refine the structure. The remaining atoms were determined using two cycles of a cyclic refinement-difference-Fourier map procedure. The structure and reflections were then transformed to the monoclinic setting using the program XTRANS and the atom list reduced. One sulfur atom, S(11), was found to lie 0.946(1) Å from itself and was refined at half-occupancy. All atoms were refined anisotropically and the structure was refined to convergence with $R(F) = 5.20\%$, $wR(F^2) = 10.75\%$ and GOF = 1.094 for all 2286 unique reflections [$R(F) = 3.92\%$, $wR(F^2) = 10.00\%$ for those 1880 data with $F_o > 4(F_o)$]. A final difference-Fourier map possessed several large peaks within 1 Å of the lanthanum atoms with $|\Delta\rho| \leq 1.97$ e Å^{-3}; the remainder of the map was essentially featureless.

Powder X-ray Refinements. Powder X-ray diffraction data were collected at 25 °C on a Rigaku $\theta-\theta$ (Cu Kα) diffractometer in the $10° \leq 2\theta \leq 60°$ range with a step width of 0.02°. The data were analyzed using an MDI software system. Cell refinement calculations were performed on all data and corrected for zero-point error. Rietveld analyses were performed with the MDI program RIQAS using split Pearson VII profile shape functions. The initial atomic coordinates and cell constants were obtained from the single-crystal studies of the respective compounds and both analyses were refined using similar algorithms. Initial structural analysis involved the refinements of the structure factors, lattice parameters, zero point and preferred orientation terms (March model), the background coefficients, and peak shape parameters. The positional parameters and isotropic thermal parameters for all atoms were refined in the latter cycles. The occupancies were fixed at the values obtained from the single-crystal experiments. Refinements of both phases yielded some negative isotropic thermal parameters that were fixed at +0.1 in the last cycles. Because of the marginal crystallinity and the overlapping impurity peaks in both samples, the resulting R_{Bragg} factors were high. The refined cell volumes for both phases differ from those obtained from the single-crystal studies. However, the fractional coordinates were essentially unchanged from the single-crystal results.

(15) Donohue, P. C. *J. Solid State Chem.* **1975**, *12*, 80.
(16) *Incomensurate Sandwiched Layered Compounds*; Meerschaut, A., Ed.; Trans Tech Publishers: Zurich, 1992; Vol. 100−101.
(17) Brese, N. E.; O'Keeffe, M. *Acta Crystallogr.* **1991**, *B47*, 192.
(18) Gabe, E. J.; Page, Y. L.; Charland, J.-P.; Lee, F.; White, P. S. *J. Appl. Crystallogr.* **1989**, *22*, 384.
(19) Sheldrick, G. M. *Acta Crystallogr.* **1990**, *A46*, 467.

Table 1. Summary of Single-Crystal and Powder (Rietveld Refinement) X-ray Diffraction Studies for $Sr_{5.8}La_{4.4}Ti_{7.8}S_{24}O_4$ and $La_{14}Ti_8S_{33}O_4$[a,b]

formula	$Sr_{5.8}La_{4.4}Ti_{7.8}S_{24}O_4$		$La_{14}Ti_8S_{33}O_4$	
formula weight (amu)	2330.64		3449.92	
space group	*P*4/*mmm*		*C*2/*m*	
a (Å)	10.569(3) [10.508(1)]		14.904(1) [14.906(1)]	
b (Å)	10.569(3) [10.508(1)]		14.736(1) [14.828(1)]	
c (Å)	8.516(4) [8.424(1)]		12.278(1) [12.280(1)]	
β (deg)	90		112.773(5) [112.436(4)]	
V (Å^3)	951.4(5) [930.1(2)]		2486.2(3) [2508.7(2)]	
T (K)	153(2) [298]		153(2) [298]	
Z	1		2	
ρ_{cal} (g/cm^3)	4.068 [4.162(1)]		4.608 [4.609(1)]	
no. of reflns	1284		4594	
no. of unique reflns	693		2287	
no. of unique reflns w/$F_o > 4\sigma(F_o)$	553		1880	
no. of variables	56		156	
radiation (Å)	0.710 73 (Mo Kα) [1.5406] [(Cu Kα)]		0.710 73 (Mo Kα) [1.5406] [(Cu Kα)]	
μ (mm^{-1})	1.449		14.333	
R[b]	4.28	[11.91]	3.92	[8.77]
$_wR$[b]	10.39	[13.65]	10.00	[8.74]
R_{Bragg}[c]		[11.20]		[18.17]
GOF	1.032		1.094	

[a] Values in brackets are from Rietveld refinements of powder XRD data. [b] For single-crystal refinements, $R = R(F) = [\sum(F_o - F_c)/\sum(F_o)]$ and $_wR = {}_wR(F^2) = [\sum w(F_o^2 - F_c^2)/\sum w(F_o^2)]^{1/2}$ for data with $F_o > 4\sigma(F_o)$. For Rietveld refinements, $R = [\sum(P_o - P_c)^2/\sum(P_o)^2]^{1/2}$ and $_wR = [\sum w(P_o - P_c)^2/\sum w(P_o)^2]^{1/2}$. [c] $R_{Bragg} = [\sum(F_o - F_c)/\sum(F_o)]$.

Results

A. Synthesis and Characterization. The compounds $Sr_{5.8}La_{4.4}Ti_{7.8}S_{24}O_4$ and $La_{14}Ti_8S_{33}O_4$ were prepared from the elements and binaries at 925−950 °C. Oxygen was introduced in the reactions by using stoichiometric additions of either TiO_2 or La_2O_3 (or SrO for $Sr_{5.8}La_{4.4}Ti_{7.8}S_{24}O_4$). Single crystals were obtained only in the presence of $LaCl_3$ fluxes (or $SrCl_2$ for $Sr_{5.8}La_{4.4}Ti_{7.8}S_{24}O_4$). The compounds were characterized by single-crystal X-ray diffraction (XRD), powder XRD (Rietveld profile analysis), and energy-dispersive X-ray analysis (EDX). The EDX studies of multiple single crystals from different preparations showed all of the constituent elements in approximately the same concentrations, but quantitative analysis was hampered by the overlap of La and Ti peaks. Initial syntheses of the $Sr_{5.8}La_{4.4}Ti_{7.8}S_{24}O_4$ and $La_{14}Ti_8S_{33}O_4$ phases involved adventitious incorporation of oxygen in the synthesis of the $Sr_{0.60}La_{0.40}TiS_3$ and $Sr_{0.20}La_{0.80}TiS_3$ phases, respectively.

Because of the serendipitous initial syntheses of the compounds, the complicated disorder problems and multiple site occupancies associated with $Sr_{5.8}La_{4.4}Ti_{7.8}S_{24}O_4$ (see next section), bulk syntheses of both phases were necessary to confirm the compositions and structural models. Attempted bulk preparations in the absence of fluxes yielded poorly crystalline samples with large impurity concentrations. However, in the presence of $LaCl_3$ fluxes, essentially single-phase samples were obtained in both cases. The compositions and compound identities of the two phases were confirmed by successful Rietveld profile refinements of the XRD data as shown in Figure 1. An unidentified impurity phase (darkened peaks, Figure 1a) is present in $Sr_{5.8}La_{4.4}Ti_{7.8}S_{24}O_4$. The Rietveld refinements of both phases gave high final residuals presumably due to the marginal crystallinity of the powder samples and the small impurities. However, the refinements clearly confirm the bulk preparations of the compounds and indicate solid solution formation (see Discussion). These data and the EDX studies suggest that there are slight differences in composition between various crytallites in the samples and that there is a compositional range for this structure type.

Table 2. Selected Bond Lengths (Å) and Angles (deg) for $Sr_{5.8}La_{4.4}Ti_{7.8}S_{24}O_4$[a]

R(1)−O(1)	2.595(7)	Ti(4)−S(1) 2×	2.327(5)
R(1)−S(6)	2.873(3)	Ti(4)−S(4) 4×	2.468(4)
R(1)−S(2) 2×	3.0042(12)	Ti(3)−O(1) 2×	1.944(7)
R(1)−S(1)	3.0546(10)	Ti(3)−S(3) 2×	2.328(3)
R(1)−S(4) 2×	3.1590(10)	Ti(3)−S(5) 2×	2.603(4)
R(1)−S(3) 2×	3.1665(9)	O(1)−Ti(3)−O(1)	167.9(5)
M(2)−S(6) 4×	2.677(5)	S(3)−Ti(3)−S(3)	101.7(2)
M(2)−S(5) 2×	2.773(6)	S(3)−Ti(3)−S(5)	94.37(13)
M(3)−S(4) 2×	2.816(4)	O(1)−Ti(3)−S(5)	85.1(2)
M(3)−S(3) 4×	2.971(3)	S(5)−Ti(3)−S(5)	69.6(2)
Ti(1)−S(2) 2×	2.443(3)	Ti(3)−O(1)−Ti(3)	102.1(5)
Ti(1)−S(3) 4×	2.464(3)		

[a] R(1) is 44% Sr and 56% La; M(2) is 42% Ti and 58%Sr; M(3) is 16% Ti and 84% Sr.

B. Solid-State Structures. *General.* $Sr_{5.8}La_{4.4}Ti_{7.8}S_{24}O_4$ is tetragonal, space group *P*4/*mmm*, and summaries of the single-crystal and powder (Rietveld) XRD refinements are given in Table 1. Selected bond distances and angles from the single crystal study are given in Table 2. The structural refinements were complicated by the presence of three mixed atom sites; two octahedral $Sr_{1-x}Ti_xS_6$ sites and one nine-coordinate $Sr_{1-x}La_xOS_8$ site. The occupancy constraints used in the final structural model in the single-crystal study required (a) full net occupancy at all three sites and (b) a summed net charge on the Sr^{2+}, La^{3+}, and Ti^{4+} cations equaling that of the S^{2-} and O^{2-} anions (i.e., a neutral compound). The occupancies in the Rietveld refinements were fixed at the values obtained from the single-crystal study. Assignment of the Ti^{4+} valency was based on the successful refinements of the XRD data. Structural models employing lower valent Ti (i.e., higher La:Sr ratios) gave substantially poorer residuals. Additional support for the refined occupancies at the three mixed-atom sites is found in an analysis of the observed bond distances and subsequent bond valence calculations. These parameters and analyses will be discussed in detail in the next section.

The structure of $Sr_{5.8}La_{4.4}Ti_{7.8}S_{24}O_4$ can be viewed as $^2_\infty[(Ti_4S_2O_4)(TiS_6)_{4/2}]^{-12}$ oxysulfide layers and $^2_\infty[Sr_{2.2}$-

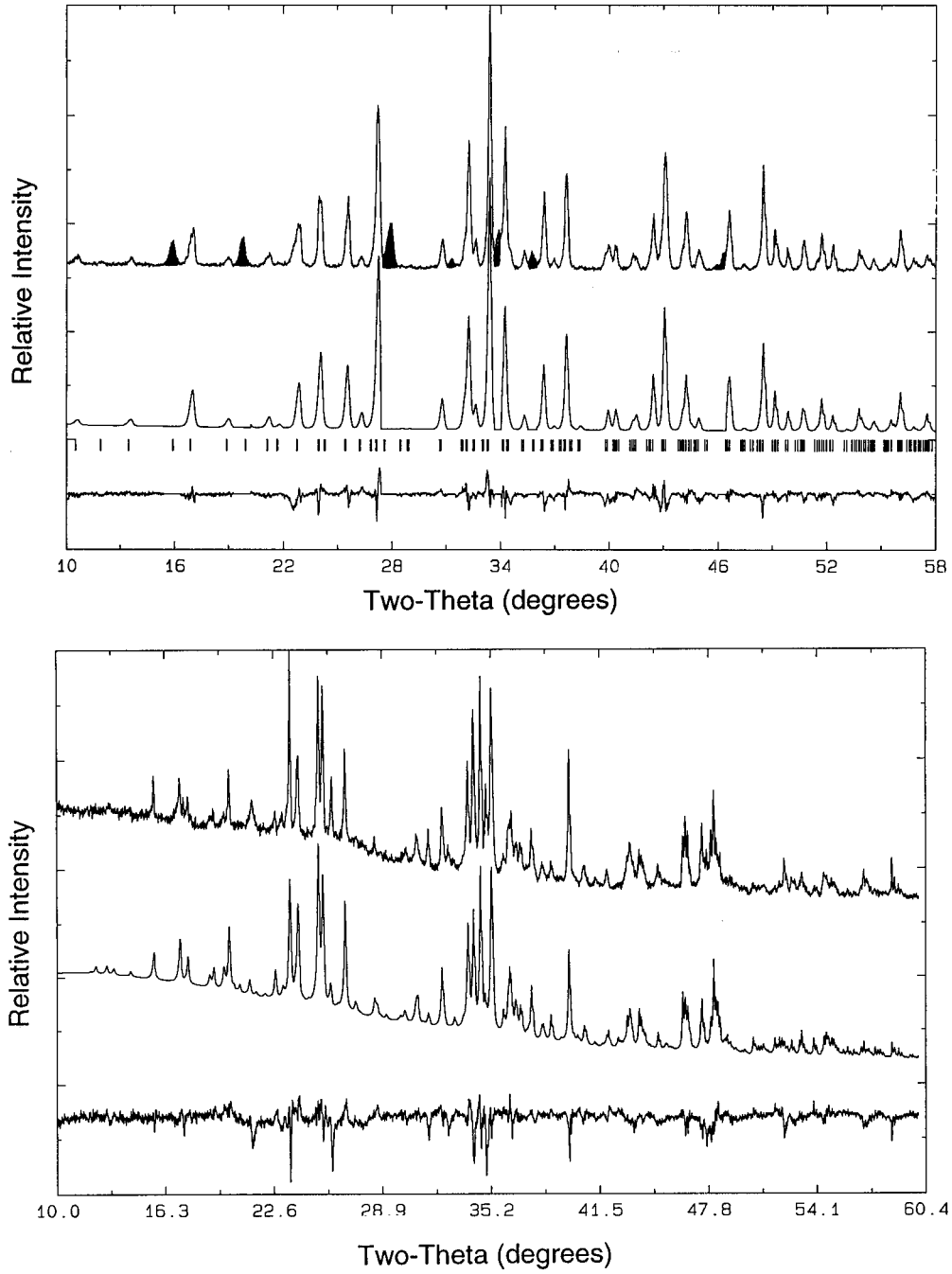

Figure 1. (a, top) Rietveld profile analysis for $Sr_{5.8}La_{4.4}Ti_{7.8}S_{24}O_4$ showing the observed (top), calculated (middle), and difference (bottom) diffraction patterns. (b, bottom) Rietveld profile analysis for $La_{14}Ti_8S_{33}O_4$ showing the observed (top), calculated (middle), and difference (bottom) diffraction patterns. The verticle bars represent allowed peak positions.

$Ti_{1.8}S_{10}]^{8.4-}$ disordered layers that alternately stack along the *c*-axis of the unit cell (see Figure 2a). The two layers are linked by several common vertexes and edges resulting in sulfur-bridged corner-sharing and edge-sharing octahedra that form a highly connected three-dimensional structure. The structures of the individual layers will be presented in the next sections.

$La_{14}Ti_8S_{33}O_4$ is monoclinic, space group $C2/m$, and has also been structurally characterized by both a single-crystal XRD study and Rietveld profile analysis of the powder XRD data. A summary of the crystallographic data is given in Table 1, and selected bond distances and angles from the single crystal study are given in Table 3. This structure also contains $^2_\infty[(Ti_4S_2O_4)(TiS_6)_{4/2}]^{-12}$ oxysulfide layers stacked normal to the $a-b$ plane in the unit cell as shown in Figure 2b. However, the oxysulfide layers in this compound are separated by isolated TiS_6 octahedra and LaS_8 and LaS_9 polyhedra that form a layer of composition $^2_\infty[La_6Ti_2S_{19}]^{-12}$.

The Common $^2_\infty[(Ti_4S_2O_4)(TiS_6)_{4/2}]^{-12}$ *Layers.* Despite the differences in crystal symmetry and compound compositions, the $^2_\infty[(Ti_4S_2O_4)(TiS_6)_{4/2}]^{-12}$ layers in the two oxysulfides are essentially identical. A projection of this layer as viewed down the *c* axis of $Sr_{5.8}La_{4.4}Ti_{7.8}S_{24}O_4$ is given in Figure 3a. The layer contains $Ti_4S_2O_4$ clusters (Figure 4) oriented such that the capping μ_4-sulfur atoms S(5) reside on the *c* axis of the unit cell (the 4-fold rotation axis). The clusters are linked in the $a-b$ plane by sharing edges with the $Ti(1)S_6$ octahedra to form an infinite square net of formula $^2_\infty[(Ti_4S_2O_4)(TiS_6)_{4/2}]^{-12}$. The $Ti(1)S_6$ octahedra

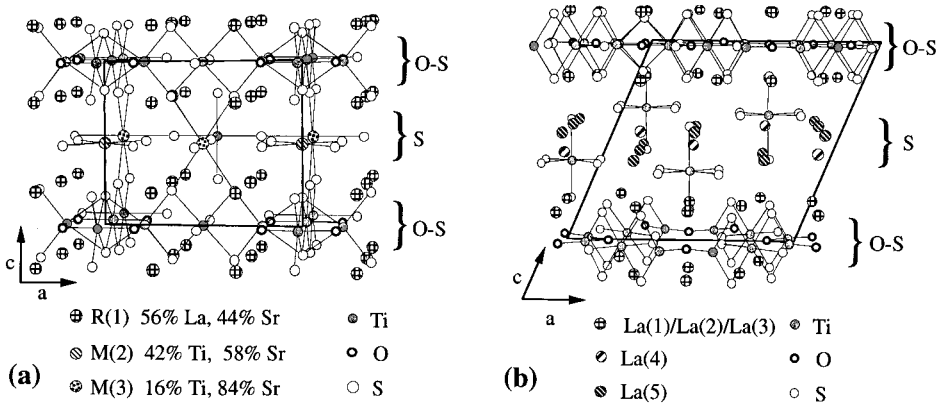

Figure 2. (a) Approximate (100) projection of $Sr_{5.8}La_{4.4}Ti_{7.8}S_{24}O_4$ structure showing the alternating layers along the *c* axis. (b) Approximate (010) projection of $La_{14}Ti_8S_{33}O_4$ structure showing the alternating layers along the *c*-axis. The boxes represent the unit cells, O−S denotes the $^2_\infty[(Ti_4S_2O_4)(TiS_6)_{4/2}]^{-12}$ layers, and S denotes the interleaving sulfide-only layers. For comparison, a common numbering scheme was used for both compounds.

Table 3. Bond Lengths (Å) and Angles (deg) for $La_{14}Ti_8S_{33}O_4$

La(1)−O(1)	2.494(7)	La(5)−S(6)	2.9542(10)
La(1)−S(9)	2.837(3)	La(5)−S(10)	2.973(6)
La(1)−S(8)	2.964(3)	La(5)−S(8)	3.004(3)
La(1)−S(2)	2.997(3)	La(5)−S(8)	3.046(3)
La(1)−S(7)	3.007(3)	La(5)−S(4)	3.088(3)
La(1)−S(2)	3.030(3)	La(5)−S(7)	3.167(3)
La(1)−S(1)	3.0916(8)	Ti(1)−S(2) 2×	2.447(3)
La(1)−S(3)	3.094(3)	Ti(1)−S(3) 2×	2.463(3)
La(1)−S(4)	3.141(3)	Ti(1)−S(4) 2×	2.474(3)
La(2)−O(2)	2.508(10)	Ti(2)−S(1)	2.258(5)
La(2)−S(8) 2×	2.998(3)	Ti(2)−S(8) 2×	2.476(3)
La(2)−S(2) 2×	3.044(3)	Ti(2)−S(7) 2×	2.491(3)
La(2)−S(4) 2×	3.056(3)	Ti(2)−S(6)	2.565(5)
La(2)−S(1)	3.085(4)	Ti(3)−O(2)	1.957(6)
La(2)−S(6)	3.127(4)	Ti(3)−O(1)	1.959(7)
La(3)−O(2)	2.508(10)	Ti(3)−S(3)	2.337(3)
La(3)−S(11)	2.818(5)	Ti(3)−S(4)	2.383(3)
La(3)−S(2) 2×	2.930(3)	Ti(3)−S(5)	2.608(4)
La(3)−S(7) 2×	3.005(3)	Ti(3)−S(5)	2.632(3)
La(3)−S(3) 2×	3.110(3)	Ti(3)−Ti(3)	2.976(4)
La(3)−S(1)	3.149(4)	O(2)−Ti(3)−O(1)	170.2(3)
La(4)−S(11)	2.794(5)	S(3)−Ti(3)−S(4)	102.48(12)
La(4)−S(9) 2×	2.808(3)	S(3)−Ti(3)−S(5)	92.30(12)
La(4)−S(11)	2.866(5)	S(4)−Ti(3)−S(5)	93.05(12)
La(4)−S(6)	2.896(4)	S(5)−Ti(3)−S(5)	72.2(2)
La(4)−S(7) 2×	3.063(3)	Ti(3)−S(5)−Ti(3)	107.8(2)
La(4)−S(10) 2×	3.329(6)	Ti(3)−O(1)−Ti(3)	100.5(5)
La(5)−S(9) 2×	2.860(3)	Ti(3)−O(2)−Ti(3)	99.0(4)

are quite regular with Ti−S distances of 2.46(1) Å (ave) which are typical for $Ti^{IV}S_6$ centers. However, the Ti(3) atoms in the $Ti_4S_2O_4$ clusters are in distorted TiO_2S_4 octahedral environments with bond distances of 2.603(4), 2.328(3), and 1.944(7) Å to atoms S(5), S(3), and O(1), respectively. It is interesting to note that virtually perfect but empty S_6 octahedra reside in the center of the square nets and are defined by four S(2) atoms and two S(1) atoms (from neighboring layers).

The $^2_\infty[(Ti_4S_2O_4)(TiS_6)_{4/2}]^{-12}$ layer of $La_{14}Ti_8S_{33}O_4$ (Figure 3b) is virtually identical with that just described for $Sr_{5.8}La_{4.4}Ti_{7.8}S_{24}O_4$ except the 4-fold symmetry is not crystallographically imposed. The *a* and *b* lattice parameters differ by only 0.17 Å and are related by a factor of $\sim\sqrt{2}$ to the *a* lattice parameter of $Sr_{5.8}La_{4.4}Ti_{7.8}S_{24}O_4$. The $Ti_4S_2O_4$ clusters are centered at a site of 2/*m* symmetry with O(1) and the capping μ_4-sulfur atoms S(5) residing on the mirror plane with the O(2) atoms residing on the 2-fold axis. The interleaving $^2_\infty[La_6Ti_2S_{19}]^{12-}$ layers (see below) are responsible for the lower crystal symmetry and cause a 4.75 Å shift between successive $^2_\infty[(Ti_4S_2O_4)(TiS_6)_{4/2}]^{-12}$ layers in the *a* direction. The metric parameters, however, show a slight lengthening of all Ti−O and Ti−S bonds relative to $Sr_{5.8}La_{4.4}Ti_{7.8}S_{24}O_4$, which may reflect the different packing forces caused by the different interlayer compositions (see Tables 2 and 3).

The $^2_\infty[Sr_{2.2}Ti_{1.8}S_{10}]^{8.4-}$ Layer in $Sr_{5.8}La_{4.4}Ti_{7.8}S_{24}O_4$. The $[(Ti_4S_2O_4)(TiS_6)_{4/2}]^{-12}$ layers in $Sr_{5.8}La_{4.4}Ti_{7.8}S_{24}O_4$ are separated by a disordered layer containing one Ti(4)S_6 octahedron, one M(2)S_6 octahedron (M(2) = 42% Ti, 58% Sr) and two M(3)S_6 octahedra (M(3) = 16% Ti, 84% Sr). Omitting the sulfur atoms shared with neighboring layers, the general composition of this layer becomes $[Sr_{2.2}Ti_{1.8}S_{10}]^{8.4-}$. The nine-coordinate tricapped trigonal prismatic holes in between the two types of layers (the R(1) site) are filled by Sr^{2+} (44%) and La^{3+} (56%) in a disordered fashion. The occupancies of the M(2), M(3), and R(1) sites were refined using a correlated SUMP instruction defined such that the net charge on the three sites summed to give a neutral compound. The R(1) site is defined by eight sulfur atoms and one oxygen with an R(1)−O distance of 2.595(7) Å and R(1)−S distances that range 2.873(2)−3.167(1) Å. The Ti(4)−S distances are quite normal at 2.42 Å (ave), whereas the M(2)−S and M(3)−S distances range 2.677(5)−2.773(6) Å [2.71 Å ave] and 2.816(4)−2.971(3) Å [2.92 Å ave], respectively. The latter distances are consistent with the refined site occupancies in that they represent weighted averages of typical octahedral Sr−S distances (for SrS, d_{Sr-S} = 3.10 Å)[20] and octahedral Ti^{IV}−S distances ($d_{Ti-S} \approx$ 2.4 Å ave).[21] Moreover, the calculated bond valencies (v_i)[17] for the R(1), M(2), and M(3) sites using the refined occupancies are +2.7, +3.2, and +2.3, respectively. These values are in good agreement with the expected values of +2.6, +2.9, and +2.3. Thus, despite the complicated disorder associated with the $[Sr_{2.2}Ti_{1.8}S_{10}]^{8.4-}$ layer, *collectively* the bulk synthesis of the compound, the successful Rietveld profile analysis of the powder XRD data, the observed M−S and R−S distances, and the corresponding bond valence analyses provide strong support for the compounds' identity and the refined occupancies at the mixed-atom sites.

(20) National Bureau of Standards, JCPDF No. 8-489.
(21) Eichhorn, B. W. In *Progress in Inorganic Chemistry*; Karlin, K. D., Ed.; John Wiley & Sons: New York, 1994; Vol. 42, p 139.

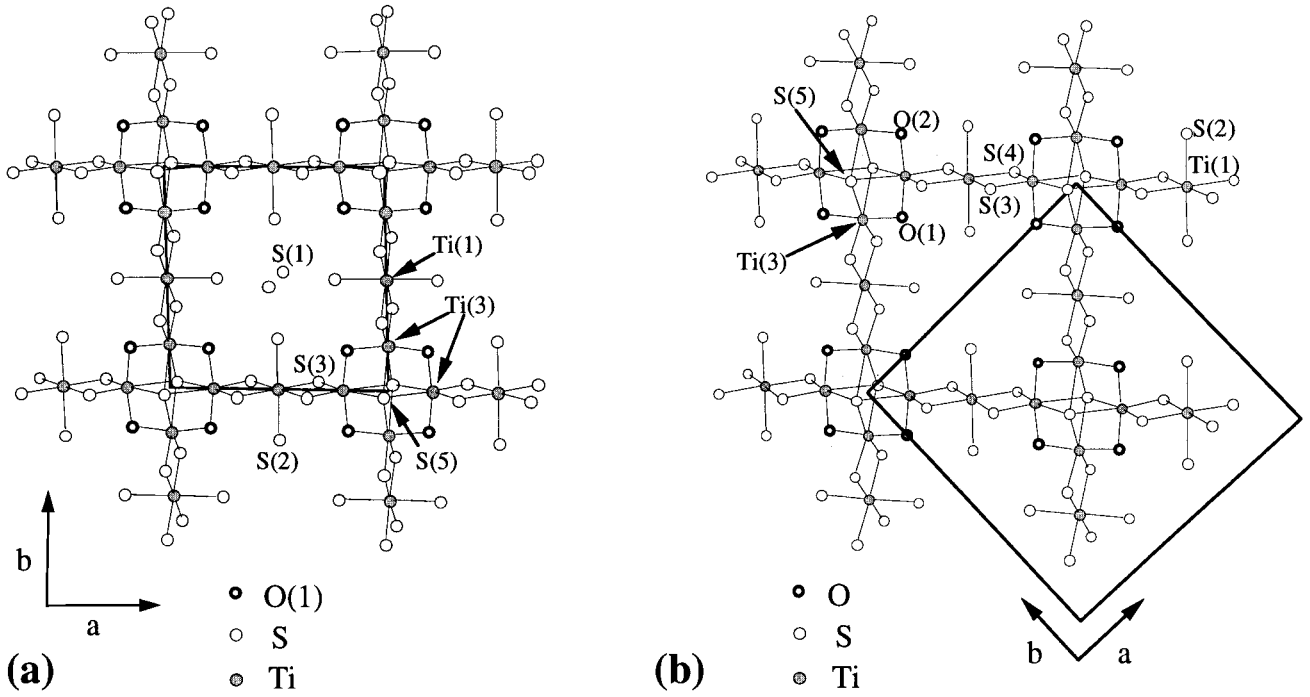

Figure 3. (a) (001) projection of the $^2_\infty[(Ti_4S_2O_4)(TiS_6)_{4/2}]^{-12}$ layer in $Sr_{5.8}La_{4.4}Ti_{7.8}S_{24}O_4$. (b) (001) projection of the $^2_\infty[(Ti_4S_2O_4)(TiS_6)_{4/2}]^{-12}$ layer in $La_{14}Ti_8S_{33}O_4$. The boxes represent the unit cells.

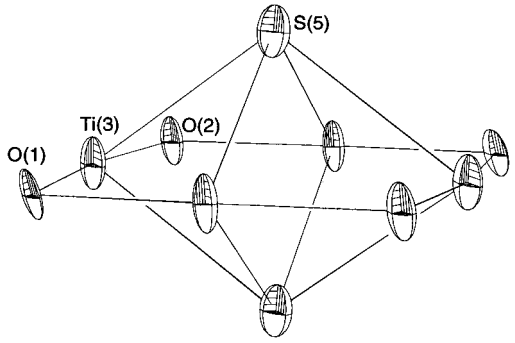

Figure 4. ORTEP drawing of the $Ti_4S_2O_4$ cluster in $La_{14}Ti_8S_{33}O_4$.

The $[Sr_{2.2}Ti_{1.8}S_{10}]^{8.4-}$ layer is defined by a central $Ti(4)S_6$ octahedron that shares its four corners in the $a-b$ plane with four $M(3)S_6$ octahedra (see Figure 5a). These corner-sharing octahedra form a two-dimensional square net in which neighboring octahedra are rotated by 45° about the Ti(4)−S(4)−M(3) vectors. The $M(3)S_6$ octahedra also share common edges with the $Ti(1)S_6$ octahedra in the $^2_\infty[(Ti_4S_2O_4)(TiS_6)_{4/2}]^{-12}$ layers to form rutile-like edge-sharing chains that run parallel to the c axis. The $M(2)S_6$ octahedra fill the holes in the square net and link the $Ti_4S_2O_4$ clusters from adjacent layers through (Ti_4O_4)−S(5)−M(2)−S(5)−(Ti_4O_4) connections that run along the c axis of the cell.

The $^2_\infty[La_6Ti_2S_{19}]^{12-}$ Layer in $La_{14}Ti_8S_{33}O_4$. For $La_{14}Ti_8S_{33}O_4$, the $^2_\infty[(Ti_4S_2O_4)(TiS_6)_{4/2}]^{-12}$ layers are separated by two isolated $Ti(2)S_6$ octahedra that are interlinked with four $La(5)S_8$ square antiprisms and two $La(4)S_9$ tricapped trigonal prisms in the $a-b$ plane. Omitting the sulfur atoms shared with the $^2_\infty[(Ti_4S_2O_4)(TiS_6)_2]^{-12}$ layers, this layer has the composition $^2_\infty[La_6Ti_2S_{19}]^{12-}$ and is shown in Figure 5b. Eight additional La^{3+} ions fill the nine-coordinate holes in between the two types of layers forming $LaOS_8$ tricapped trigonal prisms quite similar to the R(1) sites in $Sr_{5.8}La_{4.4}Ti_{7.8}S_{24}O_4$ described previously.

The $Ti(2)S_6$ octahedron is highly distorted with one short Ti−S bond of 2.258(5) Å to S(1), one rather long distance of 2.565(5) Å to S(6), and four normal contacts between 2.476(3) and 2.491(3) Å. The $Ti(2)S_6$ octahedron shares a common edge with the $La(4)S_9$ tricapped trigonal prism and a common face with the $La(5)S_8$ square antiprism. The La(4)−S contacts range 2.794(5)−3.329(6) Å whereas the La(5)−S distances range 2.860(3)−3.167(3) Å. S(11) is disordered over two sites that are 50% occupied and 0.946(12) Å apart. The range of bond distances and calculated bond valencies, Ti(2) = 3.44, La(4) = 3.42, La(5) = 3.19, are similar to those in $Sr_{5.8}La_{4.4}Ti_{7.8}S_{24}O_4$ and the other titanium oxysulfides.[6,14]

Discussion

The oxysulfides $Sr_{5.8}La_{4.4}Ti_{7.8}S_{24}O_4$ and $La_{14}Ti_8S_{33}O_4$ contain an unusual $^2_\infty[(Ti_4S_2O_4)(TiS_6)_{4/2}]^{-12}$ two-dimensional framework that is common to both phases. Moreover, the $Ti_4S_2O_4$ clusters in these layers are virtually identical with those in the $^2_\infty[(Ti_4S_2O_4)(TiS_6)_{2/2}(Ti_2S_{10})_{2/2}]^{16-}$ layers of $La_{20}Ti_{11}S_{44}O_6$[14] and other titanium oxysulfide phases.[22] The differences in the compounds are due to the replacement of the bridging $Ti(1)S_6$ unit in $La_{14}Ti_8S_{33}O_4$ for the bridging edge-shared Ti_2S_{10} bioctahedral unit in $La_{20}Ti_{11}S_{44}O_6$. In addition, the isolated $Ti(2)S_6$ octahedron in $La_{14}Ti_8S_{33}O_4$ is replaced by an isolated corner-shared $Ti_2S_{10}O$ bioctahedral fragment in $La_{20}Ti_{11}S_{44}O_6$. The recurrence of these types of layers in these vastly different compounds suggests that this linked $(Ti_4S_2O_4)$ cluster arrangement is quite stable at low oxygen concentrations and the compositions of the interlayers are less important.

(22) Tranchitella, L.; Fettinger, J. C.; Eichhorn, B. W., to be published.

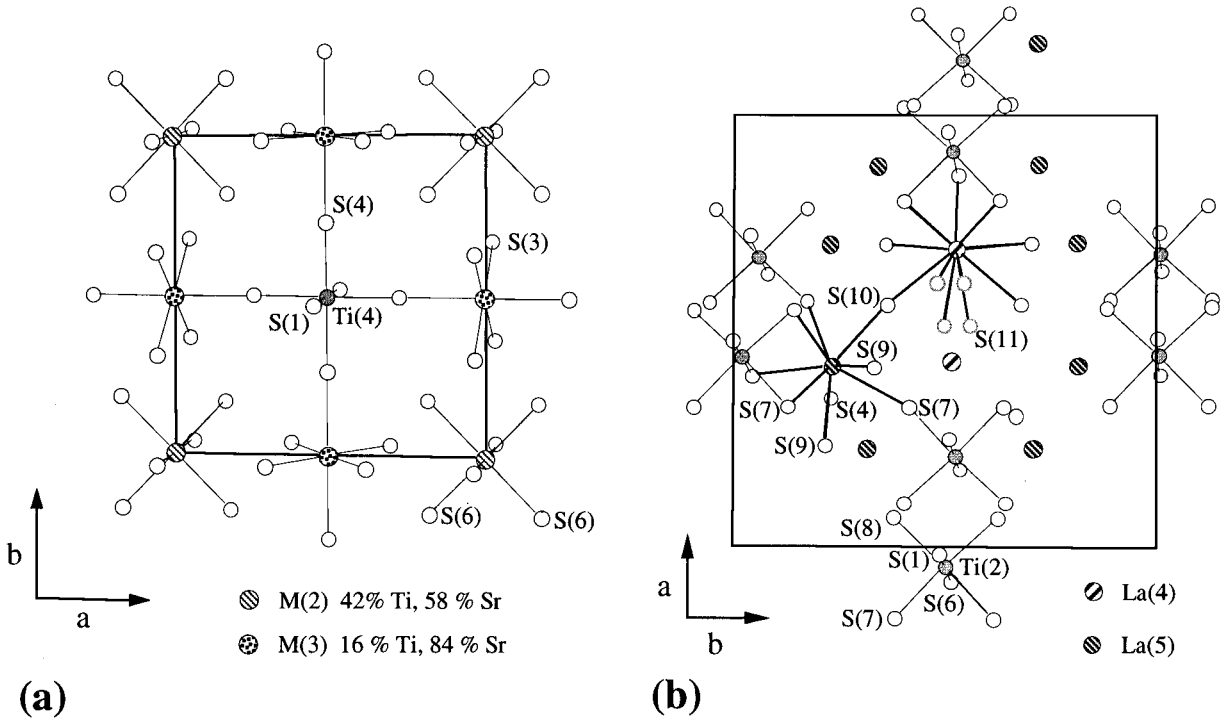

Figure 5. (a) (001) projection of the $^{2}_{\infty}[Sr_{2.2}Ti_{1.8}S_{10}]^{8.4-}$ layer in $Sr_{5.8}La_{4.4}Ti_{7.8}S_{24}O_4$. (b) An (001) projection of the $^{2}_{\infty}[La_6Ti_2S_{19}]^{-12}$ layer in $La_{14}Ti_8S_{33}O_4$. For clarity, only one of the La(4) and La(5) polyhedra are shown. The S(11) atoms are hatched and only 50% occupied. The boxes represent the unit cells.

The Rietveld refinements of the powder data confirm the bulk phase synthesis of the present compounds but the differences in the calculated lattice parameters and cell volumes between the single-crystal and powder XRD refinements in both phases may be suggestive of a solid solution formation. Recent studies[22] show that such a series does exist as evidenced by the structural characterization of $La_9Ti_9S_{24}O_4$, which is the all-lanthanum isostructural analogue of $Sr_{5.8}La_{4.4}Ti_{7.8}S_{24}O_4$. Further studies on these phases and other phases containing the $^{2}_{\infty}[(Ti_4S_2O_4)(TiS_6)_{4/2}]^{-12}$ and related layered structures are in progress.

Acknowledgment. This work was funded by the NSF-DMR and Electric Power Research Institute.

Supporting Information Available: A complete listing of Rietveld refinement data and single-crystal data including positional parameters, thermal parameters, and bond distances and angles for $Sr_{5.8}La_{4.4}Ti_{7.8}S_{24}O_4$ and $La_{14}Ti_8S_{33}O_4$ (43 pages). This material is contained in many libraries on microfiche, immediately follows this article in the microfilm version of the journal, and can be ordered from the ACS; see any current masthead page for ordering information.

CM960001J